The Journal of Experimental Biology 210, 2526-2539
Published by The Company of Biologists 2007
doi:10.1242/jeb.003939

Modulation of locomotor activity in larval zebrafish during light adaptation

Harold A. Burgess and Michael Granato*

Department of Cell and Developmental Biology, University of Pennsylvania School of Medicine, Philadelphia, PA 19104-6058, USA

*Author for correspondence (e-mail: granatom@mail.med.upenn.edu)

Accepted 3 May 2007

Summary

The neural basis of behavioral choice in vertebrates remains largely unknown. Zebrafish larvae have a defined locomotor repertoire as well as a simple nervous system and are therefore an attractive vertebrate system in which to study this process. Here we describe a high-throughput system for quantifying the kinematics of motor events in zebrafish larvae in order to measure the initiation frequency of different maneuvers. We use this system to analyze responses to photic stimuli and find that larvae respond to changes in illumination with both acute responses and extended behavioral programs. Reductions in illumination elicit large angle turns, distinct from startle responses, which orient larvae toward the source of light. In continuing darkness, larvae are transiently hyperactive before adopting a quiescent state. Indeed, locomotor activity is controlled by the state of light or dark adaptation similar to masking phenomena in higher vertebrates where light directly regulates motor activity. We propose that regulation of motor activity by photic stimuli in zebrafish larvae serves a behavioral goal of maximizing exposure to well lit environments optimal for feeding.

Supplementary material available online at http://jeb.biologists.org/cgi/content/full/210/14/2526/DC1

Key words: zebrafish, behavior, tracking, locomotion, light adaptation, visual startle, escape, masking.

Introduction

Circuit level descriptions of how sensory pathways select appropriate behavioral responses have been described in invertebrates (Kristan and Shaw, 1997; Samuel and Sengupta, 2005) but remain elusive in vertebrates. A key factor facilitating the success of analyses in invertebrates has been the ability to quantify directly the initiation and modulation of intrinsic motor patterns. Objective quantification is complicated in higher vertebrates by the enormous complexity and diversity of the locomotor repertoire. However, the sophisticated behavioral repertoire of adult animals is built upon a more limited set of simple early behaviors, hard-wired into the brain during embryonic development. These genetically encoded sensory–motor interfaces must be sufficient to enable the developing organism to locate a secure and nourishing environment, and to detect and avoid predators.

The relative simplicity of the juvenile brain and restricted set of behaviors in young animals offer advantages for studying behavioral selection. Similarly, it has long been recognized that the nervous system of fish offers an opportunity to study fundamental neuronal pathways without the many complex neuronal circuits elaborated in mammals (Stahl, 1977). Thus for studies of the neuronal basis of behavior, larval fish have the dual advantages of a functional nervous system of limited complexity, and phylogenetic relevance to functional neuroanatomy in mammals. Larval zebrafish perform several locomotor behaviors, including the optomotor response (Clark, 1981), prey tracking (Gahtan et al., 2005; McElligott and O'Malley, 2005), phototaxis (Brockerhoff et al., 1995; Orger and Baier, 2005) and multiple modes of escape response (Kimmel et al., 1974) (H.A.B. and M.G., unpublished). These behaviors are constructed from a small repertoire of motor patterns, including routine turns (Budick and O'Malley, 2000), J-turns (McElligott and O'Malley, 2005), slow scoots (Budick and O'Malley, 2000), burst swims (Budick and O'Malley, 2000; Gahtan et al., 2005; Muller and van Leeuwen, 2004), capture swims (Borla et al., 2002) and C-starts (Kimmel et al., 1974). Descriptive level models of how different maneuvers are combined into adaptive behaviors have been reported; however, direct quantitation of motor events would facilitate elucidation of the underlying neural circuitry.

Visually guided behaviors, including the optomotor response and predation, have been extensively studied in zebrafish (Neuhauss, 2003), but little is known about how simple changes in illumination effect larval behavior. Previous studies have described a startle response to abrupt decrements in light (Easter and Nicola, 1997; Kimmel et al., 1974), possibly in order to avoid looming predators. In addition to triggering visual startle responses (Hopf et al., 1973; Yates, 1981), in mammals photic stimuli trigger pupillary contraction (Keeler, 1927) and acutely suppress pineal melatonin synthesis (Klein and Weller, 1972; Lewy et al., 1980). It is now clear that locomotor activity in mammals is controlled by both endogenous circadian rhythms and acute light exposure (Aschoff, 1960). Light acutely

suppresses locomotor activity in nocturnal mammals, but promotes activity in diurnal mammals (reviewed in Redlin, 2001). The direct effect of light on activity is mediated by a non-image forming visual pathway, starting with melanopsin expressing intrinsically photoreceptive retinal ganglion cells (Hattar et al., 2003; Panda et al., 2003). This phenomenon, known as masking, can countermand circadian signals regulating activity levels and constitutes a parallel system for matching behavioral states with the diurnal cycle.

Most previous descriptions of the larval zebrafish motor repertoire have relied on comparing the kinematic performance of behaviors that have been classified by an observer (Budick and O'Malley, 2000; McElligott and O'Malley, 2005). Subjective classification of response types may fail to identify behaviors distinguished by subtle differences and precludes quantification of the large numbers of events desirable for measuring changes in behavior elicited by experimental manipulations. We therefore sought to automate the measurement of motor activity in zebrafish larvae and classify responses on the basis of quantitative measures of movement kinematics. We used automated analysis to measure behavioral responses to changes in illumination, examining effects on motor behavior at temporal windows ranging from milliseconds to hours. Our data show a role for direct photic modulation of locomotor activity in zebrafish larvae, similar to masking phenomena in higher vertebrates, and reveal a novel motor pattern elicited by sudden decrements in light intensity.

Materials and methods

Fish maintenance and breeding

Zebrafish *Danio rerio* larvae used in this study were from intercrosses of TLF (Tuebingen long fin) strain parents. Embryos were collected in the morning and thereafter maintained at 28°C on a 14 h:10 h light:dark cycle. Larvae were raised in 6 cm plastic Petri dishes at a density of 30/7 ml in E3 medium (5 mmol l^{-1} NaCl, 0.17 mmol l^{-1} KCl, 0.33 mmol l^{-1} $CaCl_2$, 0.33 mmol l^{-1} $MgSO_4$) with medium changes at 2 d.p.f. (days post fertilization) and 4 d.p.f. Behavioral experiments were conducted at 6–7 d.p.f.

Video recording

High speed video imaging was carried out with a Motionpro camera (Redlake, Tucson, AZ, USA) at 1000 frames s^{-1}, 512×512 pixel resolution, using a 50 mm macro lens. Experiments were carried out at 26–28°C in a dark room with the experimental setup further isolated by a black shroud such that light (apart from the infra-red array, below) in the testing area was <10 nW cm^{-2} (designated as 'darkness' in the text). Larvae were tested in the same 6 cm dishes as they were raised, at a density of 30/7 ml. For dark recording, larvae were illuminated using a custom built array of 50 infrared (880 nm peak) LEDs (remounted R30-123-881-120AN, Ledtronics, Torrance, CA, USA), 43 mm×50 mm in size, mounted 75 mm below the testing arena. We measured the spectrum of the infra-red LED array and found that the integral of the spectrum below 650 nm was 55 nW cm^{-2}. As the spectral sensitivity function in larval zebrafish falls off after 620 nm (Brockerhoff et al., 1997) it is unlikely that the infra-red LED array provided significant visual stimulation. Consistent with this, Brockerhoff et al. noted that no optokinetic response is elicited by infrared light (Brockerhoff et al., 1995).

Behavioral assays

Unless otherwise specified, all larvae were tested after being light adapted for at least 3 h at ~65 μW cm^{-2}. To ensure even exposure to light before testing, each plate was illuminated from below by a separate LED on a custom built light board with control of intensity using sheets of GamColor neutral density filters (GAM, Los Angeles, CA, USA). The light sources in all experiments were 5 mm white LEDs (Jameco Electronics, 320531, Belmont, CA, USA), with intensity controlled by adjusting voltage of the power source and exchanging neutral density filters (Newport, Irvine, CA, USA). For diffusion we used 3.0 mm white acrylic (ACRY2447, Modern Plastics, Los Angeles, CA, USA) after finding minimal effect on the spectrum of transmitted light. For 'dark adaptation', larvae were maintained in constant darkness for at least 12 h. In all assays, larvae were placed on the testing apparatus 3 min before beginning the experiment to minimize effects of handling and to allow larvae to adjust to any small differences in illumination from the light board (supplementary material Fig. S1). Light intensity was measured using either a Reed LX-1102 photometer (Calright Instruments, San Diego, CA, USA) or an IL-1400A-SEL033FW radiometer (International Light, Peabody, MA, USA). Where appropriate, the magnitude of changes in illumination is indicated by the log of the ratio of the final intensity and the initial intensity (log*I*). A Stamp BS2sx microcontroller (Parallax, Rocklin, CA, USA) was used to coordinate activation of the video and light stimuli. In all behavioral assays, the duration of video recordings was either 400, 500 or 1000 ms (as indicated in the figures), either immediately after the stimulus or at designated time points. The apparatus for eliciting and measuring acoustic startle responses will be described elsewhere (H.A.B. and M.G., unpublished), but briefly, responses were elicited using a minishaker (4810, Bruel and Kjaer, Naerum, Denmark), controlled by a digital-analogue card (PCI-6221, National Instruments, Austin, TX, USA). Circuit diagrams and pBASIC programs will be provided upon request. Details of the behavioral assays used are described in the figure legends.

Kinematic analysis

All kinematic analysis software was written in the IDL Development Environment (ITT Visual Information Solutions, Boulder, CO, USA). Analysis of video sequences is accomplished in four steps.

(1) Fish are tracked using a method based on the particle tracking approach of Crocker and Grier (Crocker and Grier, 1996). A bandpass filter is applied to each image in the stack so that the head of each fish is converted to a roughly circular shape indicating a local maximum (supplementary material Fig. S2A). This position is 137±42 μm (*N*=120 larvae, mean ± s.d.) caudal to the midpoint of the eyes (and approximately 380 μm caudal to the tip of the snout) and is not significantly influenced by pigmentation pattern (supplementary material Fig. S2B) or vigorous movement (supplementary material Fig. S2C). The coordinates of all local maxima are identified in the first frame of the recording, then each maxima is

individually tracked by finding the nearest maxima in subsequent frames.

(2) The orientation of the head, body and tail segments of larvae are determined. To determine the head orientation of a fish, we find the angle that maximizes the intensity of the image along a 800 μm bar extending from the head location (Fig. 1Bi, green segment and supplementary material Fig. S2A). This is sufficient to extend to the end of the swim bladder, as bending of the body axis begins only slightly anterior to this point. We find the intensity of all 360 bars around the head point, then calculate the weighted mean of angles within 8° of the maximum intensity bar. This procedure results in a robust fit, despite minor individual variations in larval morphology as the precise length of the bar does not greatly effect the measurement. To verify this, we measured 50 larvae at peak curvature, for each larva finding the standard deviation (s.d.) of 10 orientation measurements using bars ranging from 475 to 1085 μm in length. The mean of the 50 s.d. was 3.1°,

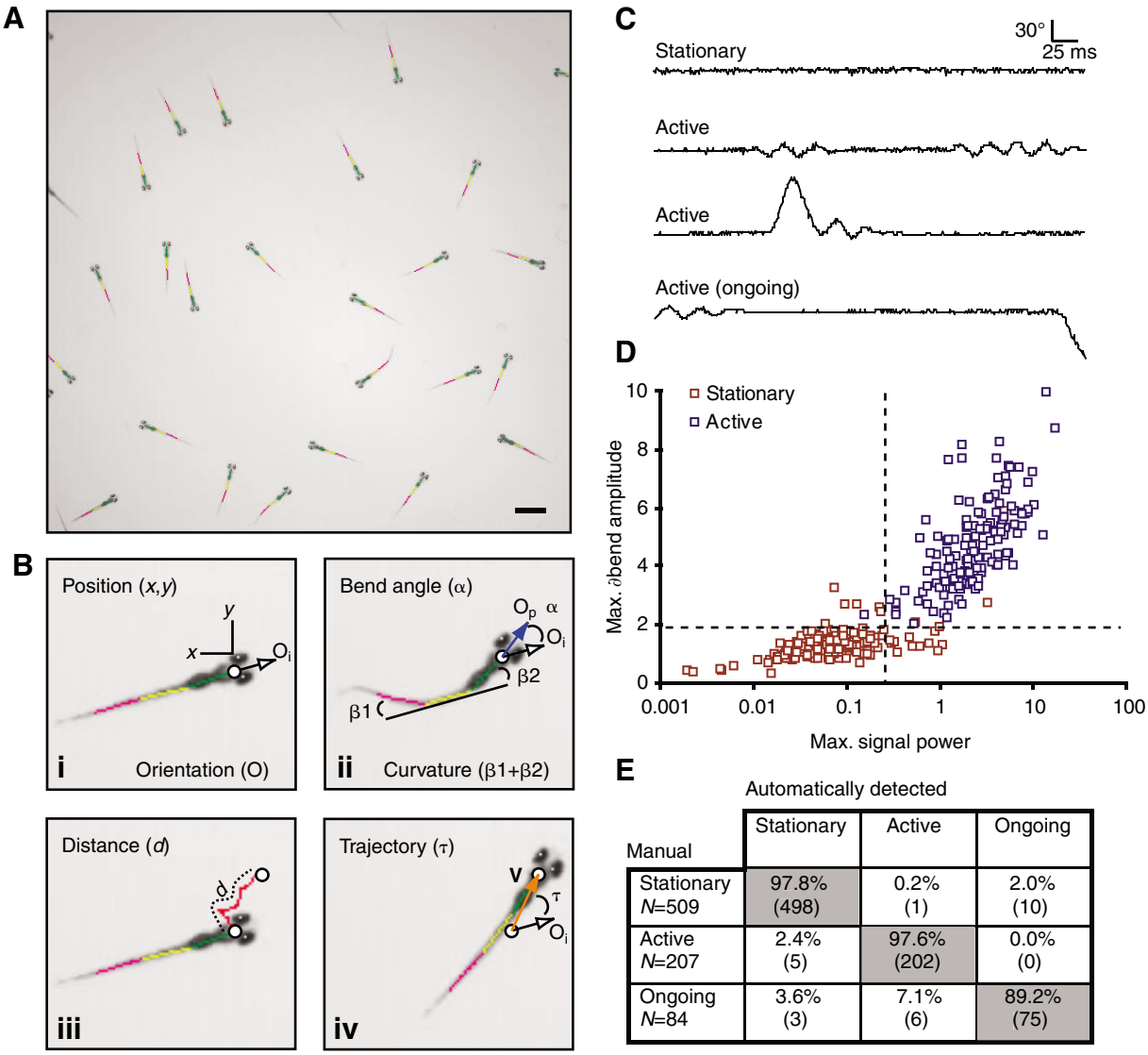

E

Manual	Automatically detected: Stationary	Active	Ongoing
Stationary *N*=509	97.8% (498)	0.2% (1)	2.0% (10)
Active *N*=207	2.4% (5)	97.6% (202)	0.0% (0)
Ongoing *N*=84	3.6% (3)	7.1% (6)	89.2% (75)

Fig. 1. High throughput measurement of locomotor kinematics in zebrafish larvae. (A) Simultaneous tracking of multiple larvae. In this example, 24 larvae are tracked over 1000 ms (red), with position and curvature information measured every ms. Scale bar, 2.0 mm. (B) Primary measurements are position, orientation (Bi) and curvature (Bii). Quantitative kinematic descriptions of locomotion are derived from these measurements, yielding measures including C-bend angle (Bii), distance traveled (Biii) and trajectory (Biv). Note that this is a high-resolution image – movement analysis is performed on the lower quality images in A. (C) Four examples showing curvature across time (400 ms). The three lower examples demonstrate the smooth changes in curvature observed for active larvae, compared to the flat curvature function for a stationary fish. (D) Scatter analysis of stationary (red squares, *N*=175) and active larvae (blue squares, *N*=156) shows that active larvae can be distinguished from stationary larvae by the maximal signal power of the Fourier transform of the curvature function, together with the maximal three-point derivative of the function. (E) Comparison of automated and manual analysis of a new group of 800 events using the criteria established in D demonstrates that automatic analysis reliably distinguishes stationary and active larvae with 98% accuracy. Larvae moving at the beginning of the video recording are detected with 90% accuracy, being mistaken for larvae initiating movement 7% of the time and stationary larvae 3% of the time. Altogether, 96.8% (775/800) events are correctly recognized.

demonstrating the robustness of this method. By repeating this process starting from the end of the first bar, we derive the orientation of the mid-body (yellow segment), and after a third iteration, of the tail (red segment). By cycling through each maxima identified in step one, orientation information is associated with position for each fish over every frame of the video recording. The use of 800 μm bars to measure body segments is empirical. Longer bars fit larvae less well at high bend angles, while shorter bars are subject to greater inter-frame variability. With this bar length, the end of the third segment lies approximately 420 μm from the tip of the tail. The low image resolution makes it difficult to accurately measure the bend angle at the tail tip, thus our measurement of larval curvature is an underestimate. However, the procedure remains robust when larvae exhibit high bend angles (supplementary material Fig. S2D) and yields sufficient curvature information to distinguish larval maneuvers (see Results).

(3) Orientation measurements across frames are used to calculate a curvature array for each fish by summation of the angles between the head/body and body/tail segments (as demonstrated in Fig. 1Bii). We use the curvature time series to analyze movement, rather than the orientation of the head alone, because during low performance swims oscillations of the tail are accompanied by very little side to side movement of the head (supplementary material Fig. S2Ei). During larger angle movements, peak head movement is closely coupled to the peak curvature (supplementary material Fig. S2Eii). The discrete Fourier transform of the curvature array is computed using the IDL fast Fourier routine to assess the presence of a signal with power above the threshold of 0.25 (as described in the Results). A bandpass smoothed curvature function is generated by inverse Fourier transform, discarding frequencies outside the range of 16 to 100 Hz. The derivative of this function is then taken as a second criteria to distinguish stationary from active fish (see Results). The first timepoint with an above-threshold curvature derivative is considered the start of movement.

(4) Maxima and minima of the smoothed curvature function are found by sliding a 5 ms window across the array beginning at the movement start time. The first maximum (or minimum depending on the direction of movement) is considered the end of the stage 1 movement.

Kinematic data are then derived from these measurements. Bend amplitude (β) is the absolute magnitude of the curvature at the first maximum/minimum. Bend angle (α) is the integral angle traversed between the initial head orientation (O_i) and the orientation at the peak of the first curvature sinusoid (O_p in Fig. 1Bii, equivalent to the C-bend angle at the end of stage 1 for C-starts). Distance (*d*) is the total path length traveled by a larva during a movement episode measured by summing the movement of the head position from frame to frame (Fig. 1Biii). Displacement (δ) is the straight-line change in the head position of the larva from the first to the last frame. Trajectory (τ) is the vector angle of movement, relative to the initial orientation of the fish. This is calculated by taking the angle between the vector (**V**) from the initial head position to the final head position and the initial orientation (O_i) of the larva (**V**–O_i in Fig. 1Biv). Other measurements include 'duration', the interval in ms from the start of movement to the peak of the first sinusoid, the 'maximal angular velocity', the greatest change in head orientation until the peak of the first sinusoid, the 'swim yaw', the mean amplitude of head swings during swimming after the first bend and counterbend (calculated by taking the average change in head orientation during each half-cycle) and the 'swim rhythm', the average peak-to-trough duration in ms of sinusoids following the initial peak/trough pair. This latter measurement is inversely proportional to tail beat frequency: tail beat frequency=1000/(2× swim rhythm). Bend angle and amplitude are used to classify movement type, as described in the text.

Larvae engaged in swimming at the beginning of a video recording (in the first 10 ms) were excluded from analysis, as were larvae initiating movement in the last 20 ms, as insufficient frames remain to determine motor pattern type. This typically resulted in elimination of 5–10% of traces from further analysis. Motor pattern kinematics cannot be measured if larvae begin a movement bout lying on their side. As recordings are made from above, the visibility of both eyes is a good surrogate for vertical posture. To find the eyes, a second bandpass operation is performed in the region centered on each head and local maxima recorded. Maxima anterior to the midpoint of the head are counted. Only larvae with two anterior local maxima are further analyzed. Generally 2–3% of larvae are excluded by this procedure. Analysis software is available upon request.

Laser ablations

To visualize reticulospinal neurons, a 50% solution of fluorescein-conjugated dextran 10 K M_r (Invitrogen, Carlsbad, CA, USA) in 10% Hanks' saline was pressure injected into the ventral spinal cord of 4 d.p.f. larvae. The next day, larvae were treated briefly with 0.03% tricaine (3-aminobenzoic acid ethyl ester, Sigma, St Louis, MO, USA) and mounted in methylcellulose or 2% low-melt agarose. Ablations were performed using a Micropoint pulsed nitrogen laser (Photonic Instruments, St Charles, IL, USA) mounted on a compound microscope (Carl Zeiss, Thornwood, NY, USA) with a 63× water lens. Cells were pulsed for 30 s at 10 Hz. Larvae were remounted after 6 h and inspected. As previously reported, after ablation the Mauthner axon stump was clearly visible in many instances (Liu and Fetcho, 1999), whereas following unsuccessful ablations fluorescence returned to the Mauthner cell. Larvae were individually tested for dark-flash and acoustic startle responses on 6 d.p.f. At the end of the experiment, larvae were fixed in 4% paraformaldehyde and stained with 3A10 antibody (1:50, kind gift of Dr T. Jessell) (Hatta, 1992) and Alexa-594 conjugated goat anti-mouse antibody (Invitrogen) to confirm complete elimination of both Mauthner cells in lesioned larvae. This procedure resulted in successful lesion of 80% of Mauthner cells targeted.

Statistical analyses

All Student *t*-tests are two-tailed, independent sample, assuming equal variance unless noted and were performed using Excel (Microsoft, Redmond, WA, USA). Analysis of variance (ANOVA) and non-linear regression analysis was carried out using SPSS 14.0 (SPSS, Chicago, IL, USA). *P* values were subjected to Bonferroni correction to maintain alpha=0.05. Gaussian fitting was carried out using D. Lindler's *xgaussfit* tool for IDL. Spectral analysis of ultraradian time series was

performed using the fast Fourier transform implementation in IDL. Time constants were estimated by fitting data with a single exponential function using CurveExpert v1.3 (Hixson, TN, USA). Values are means ± s.e.m., except where otherwise noted.

Results

High throughput measurement of motor behaviors

To study a broad range of motor behaviors, we adapted a system previously built to measure startle responses (H.A.B. and M.G., unpublished). First, video recordings of groups of day 6–7 larvae are acquired at 1000 frames s^{-1}. Then using a multi-particle tracking algorithm, we determine the position of individual larvae across consecutive frames, allowing us to track the movement path of up to 30 larvae simultaneously (Fig. 1A). The 'position' of a larva represents the location of its maximal optical density, and corresponds to a point in the middle of the head behind the eyes. We define the curvature of the larva using a similar measure to the 'Head–Tail' angle of Budick and O'Malley (Budick and O'Malley, 2000), by adding the angles made by the head and tail with the mid-body segment (Fig. 1Bii). Plotting the curvature of a fish over time reveals smooth oscillations reflecting the sinusoidal motion of swimming (Fig. 1C).

To find criteria by which movement bouts could be distinguished from stationary episodes, we manually identified

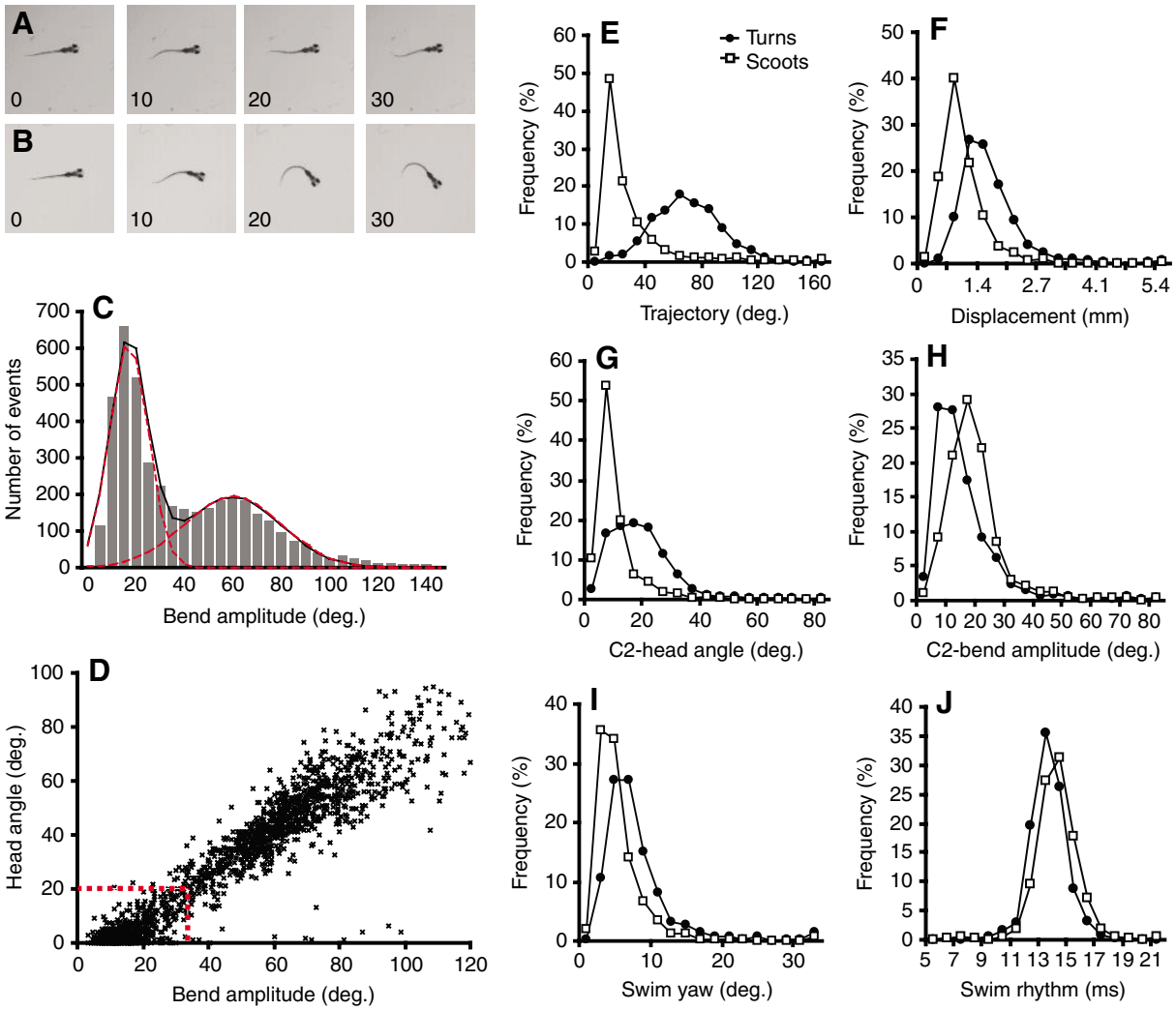

Fig. 2. Kinematic identification of the two most frequently observed elements of the larval locomotor repertoire, scoots and routine turns. (A) Example of a scoot, showing the low bend angle and forward trajectory of the larva. (B) Example of a routine turn, demonstrating the large bend angle and reorientation of the larva prior to forward swimming. (C) Histogram of bend amplitudes for 4199 movement events. The histogram was fitted as the sum of two Gaussians (solid black line: for peak 1, μ=16.9, σ=7.9; peak 2, μ=59.6, σ=20.1). (D) Scatter analysis of bend angles against bend amplitudes for 1681 movement episodes confirms spontaneous motor events do not form a behavioral continuum, but can be distinguished by selecting thresholds for bend amplitudes and angles. Red dotted line indicates the amplitude and head bend angle thresholds used to distinguish scoots from turns. (E–J) Kinematic analysis of the two types of movement events distinguished in D (672 scoots, 1009 turns) verifies that this method identifies motor patterns with distinct properties. Kinematic distributions for trajectory (E), displacement (F), head bend angle for the second sinusoid, equivalent to the 'counterbend' for turns (G), bend amplitude for the counterbend (H), swim yaw (I) and swim rhythm (J) show highly significant differences (independent sample *t*-test with unequal variances, $P<10^{-10}$).

Table 1. *Automated classification of larval motor patterns*

Observed	Automatically (auto) classified			Total observed
	Stationary	Turn	Scoot	
Stationary	337	2	7	346 (57.7%)
Turn	0	124	6	130 (21.7%)
Scoot	4	4	116	124 (20.7%)
Total auto classified	341 (56.8%)	130 (21.7%)	129 (21.5%)	

175 stationary traces, and 156 examples of spontaneous movements. As anticipated, the maximal signal power of the fast Fourier transform of the curvature function was significantly greater in moving fish than in stationary fish. The derivative of the curvature function also distinguished moving and stationary fish. Stationary fish could be distinguished from active fish with 97.9% accuracy (324/331) using a signal power threshold of 0.25 and a derivative threshold of 2.0 (Fig. 1D). The earliest time point at which the curvature function exceeded the threshold was designated as the onset of a movement episode. We validated these criteria using a separate set of 800 manually categorized curvature traces (Fig. 1E). For the 202 active larvae whose latency was determined both automatically and manually, the major discrepancy was that for 28 larvae, the computer failed to identify the first oscillation of 'on-the-spot' wiggles of the tail or low performance swim bouts. In these cases, subsequent cycles were picked up and the event correctly classified as a scoot due to the small head angle and bend amplitude (see below). In one case, the fish performed two distinct movements and the initiation of the second was correctly identified while the first was missed. For 166 of the remaining 173 larvae (96%), the automatically determined initiation time was less than 9 ms from the observed time (median 2 ms, inter-quartile range 0–3 ms). As the duration of routine turns is greater than 10 ms (24–34 ms at 22°C in (Budick and O'Malley, 2000) and 15.7±3.7 ms in our measurements at

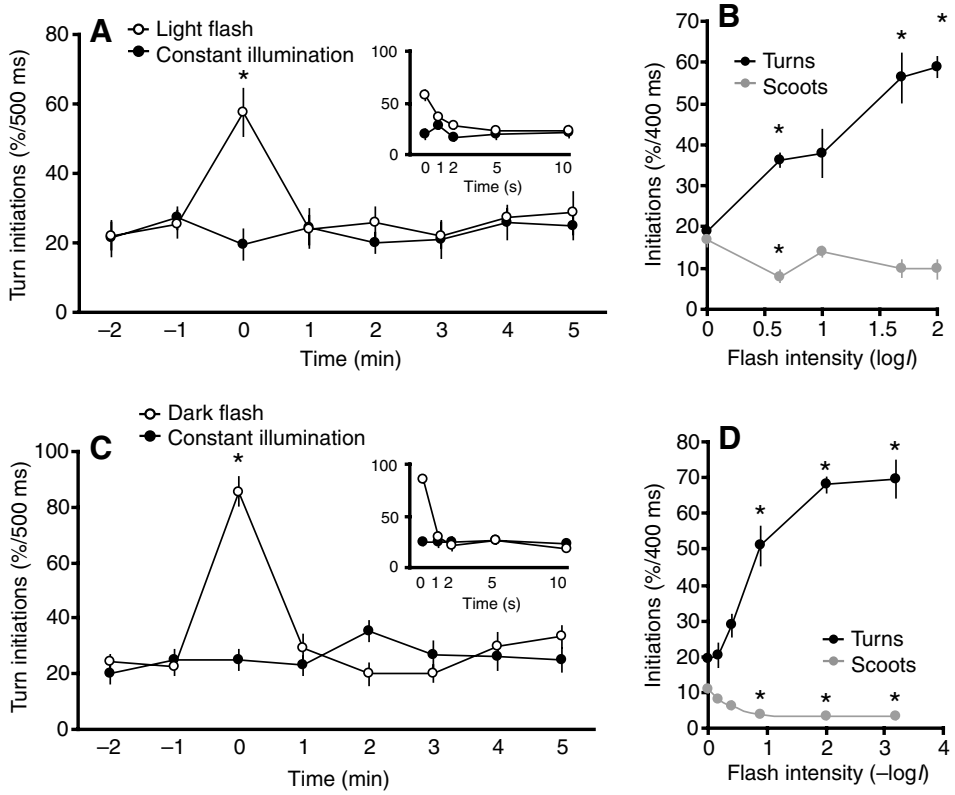

Fig. 3. Locomotor responses to light and dark flash stimuli. (A) Transient increases in light elicit a sharp spike in turn initiations. Larvae were pre-adapted at 20 μW cm^{-2} white light and at time zero, tested with a 500 ms pulse of 200 μW cm^{-2} (open circles, N=8 groups) or maintained in constant illumination (closed circles, N=8 groups). Activity was measured in 400 ms windows at the indicated time points. A significant spike in turns was noted for the time window coinciding with the light flash (two-tailed t-test, P=0.0064) but not at any other time points. Scoot initiations were not significantly altered by the light-flash (data not shown). (B) Turn initiations (black circles) increase with the intensity of the light flash. Larvae were pre-adapted at 20 μW cm^{-2} before being tested with a series of 10 bright flashes at the indicated intensity levels, at 30 s intervals (N=5 sets of larvae for each intensity). A significant increase in the frequency of turn initiations compared to baseline levels was found for light flashes of >1 log unit above baseline illumination (*P<0.05). Scoot initiations (grey circles) in the same larvae were slightly depressed compared to baseline, but this only achieved significance at one intensity tested. (C) Transient decreases in light provoke an increase in turn initiations. Larvae were pre-adapted at 200 μW cm^{-2} and challenged with a 500 ms-long dark flash to 20 μW cm^{-2} at time zero (open circles, N=10 groups) or left in constant illumination throughout the experiment (closed circles, N=10 groups). Turns were significantly increased in the 500 ms window starting at the beginning of the dark flash (two-tailed t-test, $P<10^{-10}$), but not at any other time point. Scoots were significantly reduced only in the time window corresponding to the dark-flash, most likely reflecting the huge increase in turns at that time. Scoot initiations were otherwise not affected (data not shown). (D) Larger reductions in illumination elicit more turn responses, without evoking scoots. Larvae were pre-adapted at 130 μW cm^{-2}, then tested with a series of 10 dark flashes of the indicated magnitude (N=6 per intensity). Turn initiations (black circles) were significantly increased (*P<0.05) for dark flashes of around 1 log unit and greater whereas scoot initiations (grey circles) were reduced under the same conditions, likely as a result of the large number of larvae initiating turns.

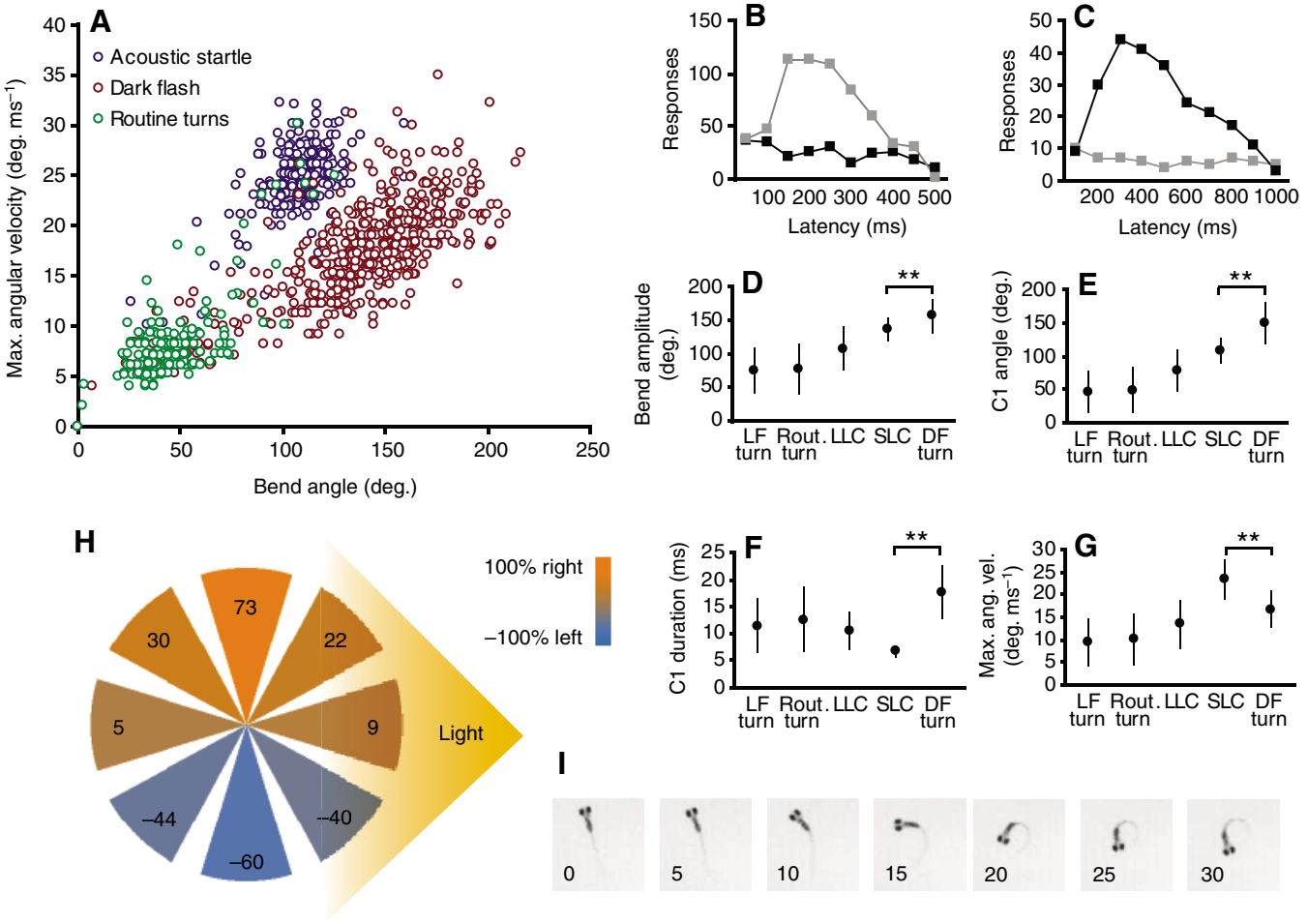

Fig. 4. Kinematic properties of turns initiated in response to changes in illumination. (A) Scatter analysis of turn kinematics for spontaneous routine turns (*N*=166, green), turns elicited by dark flashes (*N*=506, red) and short latency acoustic startle responses (*N*=269, blue). Dark-flash evoked turns form a distinct cluster, with bend angles exceeding those achieved by acoustic startle responses, but with much slower angular velocity. (B) Latency distribution for turns initiated during a 500 ms light flash (*N*=631, grey squares) or under constant illumination (*N*=244, dark squares). Turns peak around 200 ms after the increment in lighting. (C) Turns initiated in response to a 1000 ms dark flash (*N*=236, dark squares) have a longer latency, peaking 300 ms after the reduction in lighting. Turns initiated during constant illumination (*N*=63, light squares) show uniform distribution. (D–G) Comparison of movement kinematics for five motor patterns. Turns elicited by light flashes ('LF turn', *N*=111), routine turns ('Rout. turn', *N*=66), long latency acoustic startles ('LLC', *N*=96), short latency acoustic startles ('SLC', *N*=382) and turns elicited by dark flashes ('DF turn', *N*=104); values all means ± s.d. Light-flash turns were indistinguishable from routine turns for all kinematic parameters scored. Kinematics of long latency startles differed from routine turns for all kinematic parameters scored. Turns elicited by dark flashes were distinct from short latency acoustic startle responses. Although turn magnitude is extreme for dark flashes, turns are relatively slow, but occur over a protracted duration (two-tailed *t*-tests, $^{**}P<0.001$). (H) After light extinction, larvae orient toward the area where the light was extinguished. Cones represent initial orientation of larvae, shading and numbers indicate rightward turn bias (where 100% signifies that all turns are made to the right, –100% means always left). Larvae initially facing the light with their right side show a strong right turn bias, while the opposite is true for larvae in the reverse orientation. Larvae oriented parallel to the direction of the light show no directional bias. (I) Example of a dark-flash turn, demonstrating the very large bend amplitude attained and 180° reorientation typical for these motor patterns.

28°C), the accuracy is sufficient to ensure measurement of the bend amplitude at the sinusoid peak and thus distinguish turns from smaller movements. This shows that movement episodes can be reliably identified by the computer, permitting automated analysis of kinematics, using the primary measurements of position, orientation and curvature.

Two major motor patterns have been described during spontaneous movement episodes in zebrafish larvae (Budick and O'Malley, 2000). Forward directed swim bouts have been previously referred to as 'slow' or 'burst' swims, depending on the vigor of the side-to-side movements (Budick and O'Malley, 2000; Ouagazzal et al., 2001; Thorsen et al., 2004). However, as behavioral measurements suggest that the intensity of rhythmic activity during swimming constitutes a continuous variable (H.A.B. and M.G., unpublished), here we will simply refer to forward movements as 'scoots' (Fig. 2A). 'Routine turns', here referred to as 'turns', are initiated with large changes in body curvature and head angle (Fig. 2B). Indeed, the histogram of initial bend amplitudes for 4199 movement episodes initiated by larvae in the absence of extraneous

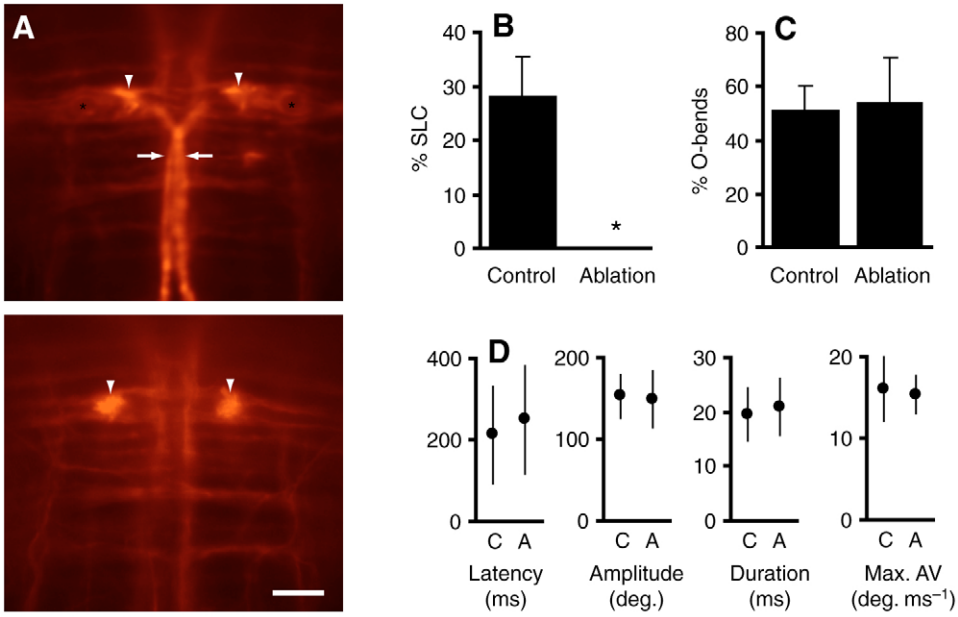

Fig. 5. Large angle C-start responses to dark-flash stimuli are Mauthner independent. (A) Laser ablation of Mauthner cells. Cell bodies (asterisks) and axons (arrows) visible in control lesions (top) are absent in immunohistochemical staining 48 h after ablation (bottom), while fibers coursing around the Mauthner cells, including the axon cap (arrowheads) are unaffected. Scale bar, 20 μm. (B) High performance startle responses elicited by acoustic/vibratory stimuli in control larvae ('control', *N*=8) are completely abolished after bilateral Mauthner cell lesion ('ablation', *N*=6 larvae). Slower, long latency responses to the same stimulus are not affected by Mauthner cell lesions (data not shown). (C) Mauthner cell ablation does not impair dark-flash responsiveness in the same set of larvae, showing that O-bend responses to dark-flash stimuli are not initiated by the Mauthner cell startle circuitry (two-tailed *t*-test, *P*=0.89). Larvae were tested individually with a series of 10 dark flash stimuli from 65 μW cm^{-2} to darkness, at 1 min intervals. (D) O-bend kinematics during the dark-flash test in control larvae ('C') and ablated larvae ('A') are almost identical, arguing that the Mauthner cell is not involved in larval dark-flash responses. No statistical differences are present between any pair of kinematic values (two-tailed *t*-test, *P*>0.1 for all measures). Values are means ± s.d. of O-bend responses.

stimulation reveals a bimodal distribution, consistent with the presence of scoots and turns (Fig. 2C). Scatter analysis of a separate 1681 spontaneous movement episodes shows that larvae initiating locomotor activity with small bend amplitudes (less than 35°) also tend to show only slight changes in head orientation (less than 20°), allowing the two types of movement to be distinguished on the basis of these two criteria (Fig. 2D).

To evaluate the accuracy of this method, we compared automated classification of behavior to classification by an observer for 600 events (Table 1). Automated classification again recognized non-moving fish with 97.3% accuracy (337/346 events), similar to our previous result. Turns were correctly identified 95.3% of the time (124/130), and scoots with 93.5% accuracy (116/124). As incorrect assignments occurred at a similar frequency for the three categories, the automatically determined rate of motor initiations was very close to the observed rate. For turns, both automated classification and manual observation yielded 21.7% initiations per 400 ms window, while for scoots, automated classification gave 21.5% compared to 20.7% for manual classification.

Analysis of kinematic parameters of movement episodes automatically classified as scoots or turns affirms that these represent distinct locomotor behaviors. Scoots are almost completely forward movements (Fig. 2E, trajectory 17±23°, mean ± s.d., *N*=672), whereas turns cause larvae to swim at an angle to their initial orientation (62±30°, *N*=1009) and result in a greater displacement (Fig. 2F, 1.57±1.17 mm for turns *versus* 0.91±0.57 mm for scoots, independent sample *t*-test $P<10^{-10}$). The second peak of the sinusoid, representing the counterbend for turns, is also different for scoots and turns (Fig. 2G,H). Following these first two components of the sinusoid, turns are followed by an average of 3.6±2.0 tail beats, and scoots by 2.8±1.8 movements. The mean yaw of scoots is slightly but significantly smaller than for turns (Fig. 2I). In addition, the average duration of tail flips (denoted 'rhythm') is slightly less in turns (Fig. 2J). Mean swim rhythm for turns and scoots is 12.6±2.7 ms and 13.7±1.7 ms, respectively, yielding tail-beat frequencies of 39.6 Hz and 36.4 Hz, respectively, in agreement with previously reported values (Borla et al., 2002; Budick and O'Malley, 2000; Muller and van Leeuwen, 2004). These results demonstrate that the two major locomotor maneuvers reported by human observers can also be identified on the basis of their distinctive kinematic properties, permitting automated analyses of behavior.

Responses of zebrafish larvae to transient changes in irradiance

We first considered the effect of transient increases in lighting for larvae pre-adapted to 20 μW cm^{-2} of white light. A 500 ms 'light flash' of 200 μW cm^{-2} evoked an increase in turn responses from 19.6±4.4% initiations per 400 ms window in baseline controls to 57.4±6.8% in the light-flashed groups (*N*=8 each condition, two-tailed *t*-test, *P*=0.0064), but no changes in the frequency of turn initiations from 1 s to 5 min after the stimulus (Fig. 3A). Scoot initiations were reduced immediately after the stimulus, likely because the larvae were instead initiating turns, but thereafter returned to baseline levels and remained stable (data not shown). More intense light elicited a greater increase in turn initiations (Fig. 3B; *N*=5 each intensity, one-way ANOVA $F_{(4,20)}$=16.4, *P*<0.001). A similar pattern was seen for brief decrements in illumination ('dark flashes' of 1 log unit intensity). A significant spike in turn initiations was observed immediately after the stimulus, from 24.9±3.6% initiations per 500 ms window in baseline controls to 86.6±5.2%

in the dark-flashed groups (N=10 each condition, two-tailed t-test, $P<10^{-10}$), with the frequency of turns returning to baseline at 1 s through 5 min after the stimulus (Fig. 3C). Scoot initiations were not affected. The acute increase in turn initiations was proportional to the magnitude of the change in illumination (Fig. 3D; N=6 each intensity, one-way ANOVA $F_{(5,30)}$=31.6, P<0.001). Thus, both sudden increases and reductions in irradiance provoke immediate turn responses.

Because abrupt sensory stimuli in a variety of modalities elicit startle responses in larval zebrafish, we next asked whether visually evoked turn responses show kinematic similarities to startle responses. Scatter analysis showed that turns evoked by dark flashes (N=506) have markedly larger bend angles relative to their angular velocity than acoustic startle responses (N=269) (Fig. 4A). Only six out of 166 routine turns achieved bend angles over 100° (Fig. 4A), and five of these instances had an

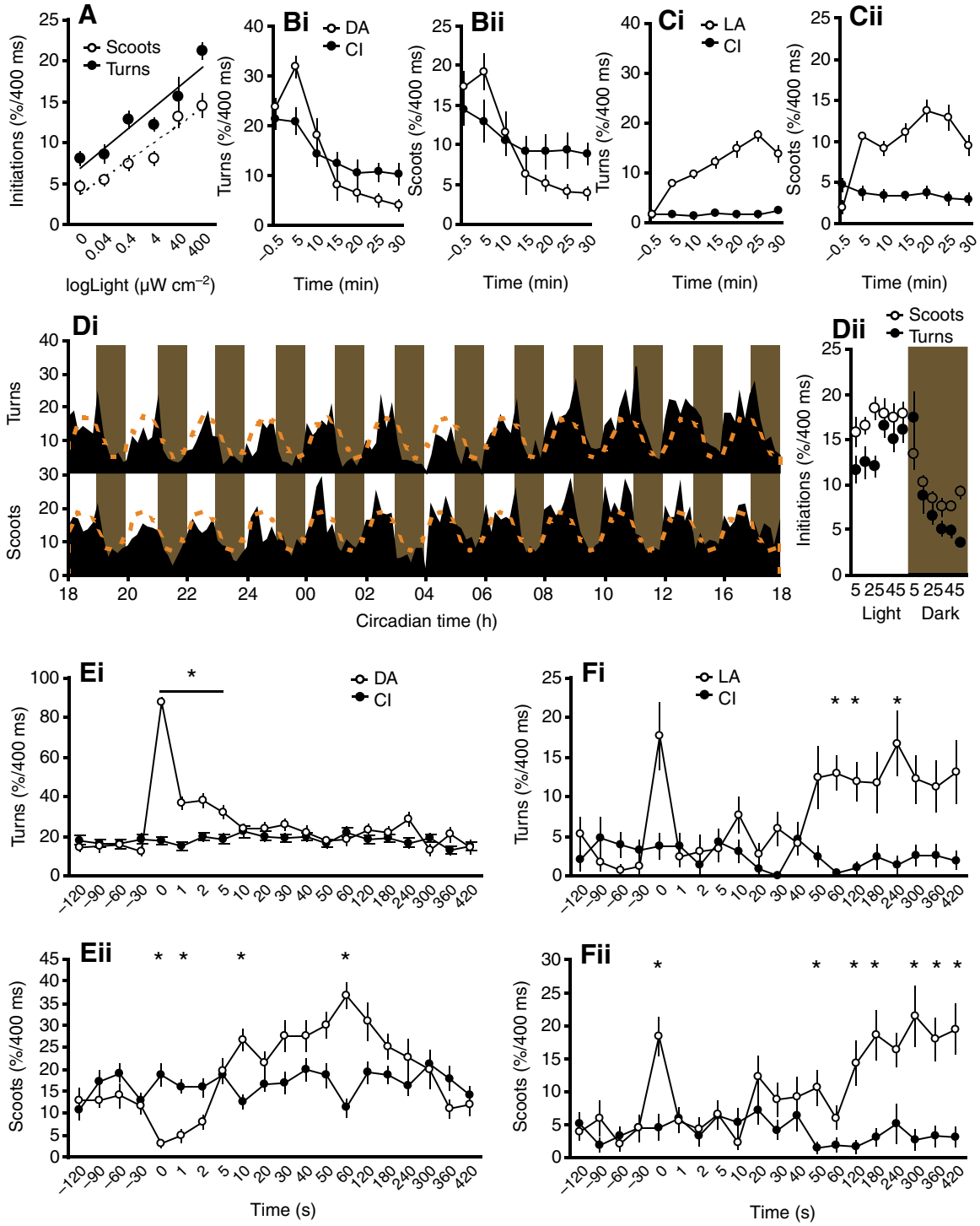

Fig. 6. See next page for legend.

angular velocity similar to that of acoustic startle responses, suggesting that the larvae may have responded to environmental cues. Acoustic and touch-evoked startle responses in zebrafish larvae are initiated within 15 ms of the stimulus (Liu and Fetcho, 1999). In contrast, turns elicited by light flashes are initiated at a latency of 183±93 ms (Fig. 4B) and turns initiated in response to dark flashes are even more delayed, with a mean latency of 408±105 ms (Fig. 4C). Response latencies are somewhat variable; in other experiments, we found that dark-flash turn latencies varied with the degree and duration of light adaptation and could be as short as 150 ms (data not shown). However, in every experiment we observed responses with latencies exceeding 500 ms. The protracted latency of visually evoked turns is unexpected and suggests that the function of these responses may not be to escape from predators.

Detailed kinematic comparison of visually evoked turns, routine turns and startle responses revealed that turns evoked by increases in illumination are indistinguishable from routine turns, showing almost identical head angle, bend amplitude, duration and maximal angular velocity of the initial C-bend (Fig. 4D–G; 'LF turn' (N=111) *versus* 'Routine turn' (N=66); t-tests yield P>0.1 for comparisons of C-bend angle, amplitude, duration and maximal angular velocity). In contrast, turns evoked by reductions in irradiance are not similar to other motor patterns, including acoustic startle responses (t-test, unequal variances, $^{**}P<10^{-10}$). Whereas acoustic startle responses are initiated with short duration (6.7±1.0 ms, mean ± s.d.), large angular velocity (23.5±4.2° ms^{-1}) C-starts, the C-bends evoked by dark flashes have a relatively slow angular velocity (16.9±4.0° ms^{-1}), but are of such exceedingly long duration (17.5±4.8 ms) that the bend amplitude and angle achieved are much larger than those recorded during acoustic startle responses (bend angle 149.5±30.0° for dark-flash responses *versus* 108.8±18.1° for acoustic startle responses). Thus, the kinematic data argues that dark-flash evoked turns represent a distinct maneuver within the larval motor repertoire.

The escape response in adult fish is directed away from threatening visual stimuli (Dill, 1974; Domenici, 2002). We analyzed turn direction according to initial orientation. Surprisingly, larvae responded to dark-flash stimuli by turning towards the position of the dimmed light (Fig. 4H). Binning orientations by quadrant, for larvae initially facing the light with their right eye, 83.9±2.5% of turns were to the right, compared to 30.2±7.6% rightward turns for larvae facing the light with their left eye (mean ± s.e.m., t-test, $P=1.8\times10^{-4}$; five groups tested with 20 dark flashes each). Hence dark-flash responses differ from visual escape responses in the direction of their trajectory.

High-performance acoustic startle responses in zebrafish larvae are mediated by the bilateral Mauthner cells (H.A.B. and M.G., unpublished). The slow kinematics of dark-flash responses suggest that Mauthner cells may not be involved in this motor pattern. To test this idea, we laser ablated both Mauthner cells (Fig. 5A) and asked whether dark-flash responses were impaired. As expected, lesion of both Mauthner cells completely eliminated short latency startle responses to acoustic stimuli (Fig. 5B). In contrast, both responsiveness (Fig. 5C; two-tailed t-test, P=0.89) and kinematics (Fig. 5D; two-tailed t-test, P>0.1 for all measures) of C-bend responses to dark-flash stimuli were indistinguishable in ablated larvae and controls, arguing against involvement of Mauthner cells in the performance of the dark-flash response. As dark-flash

Fig. 6. Locomotor activity is regulated by light. (A) The frequency of spontaneous turn (closed circles) and scoot (open circles) initiations are significantly greater in more intense light. Larvae (N=10 groups per light level) were adapted to each light level for 30 min before testing. For each group, a series of twenty 400 ms video recordings was made under constant conditions at the indicated light level and average activity computed. Regression lines for activity *versus* log(intensity) are shown (turns, r^2=0.49; scoots, r^2=0.51). (B) Both turn (Bi) and scoot (Bii) initiations show a gradual reduction during dark adaptation (DA). Larvae were pre-adapted to 400 μW cm^{-2} white light for at least 3 h before being subjected to sudden darkness (open circles, N=10 groups) or were maintained under constant illumination (CI; closed circles, N=10 groups). At each time point, a series of twenty 400 ms video recordings was made and the average activity computed for each group. Two-way ANOVA for group and time after light extinction revealed significant group by time interaction for both scoots ($F_{(5,107)}$=3.3, P=0.009) and turns ($F_{(5,107)}$=5.4, P<0.001). (C) Both turn (Ci) and scoot (Cii) initiations rapidly increase after larvae maintained in constant darkness are suddenly switched to bright light. Within 15 min of illumination with 230 μW cm^{-2} (light-adapted, LA; open circles, N=10 groups), both turn and scoot initiations reach levels similar to larvae maintained in bright light for several hours (for example, constant illumination groups in B). Control larvae maintained in constant darkness (CI, closed circles, N=10 groups) continue to show low levels of locomotor activity. Two-way ANOVA for group and time for time points after the onset of illumination revealed a significant main effect of group for both scoots ($F_{(1,107)}$=216, P<0.001) and turns ($F_{(1,107)}$=482, P<0.001), and a significant group by time interaction for turns ($F_{(5,107)}$=7.9, P<0.001). (D) Ultraradian light:dark cycles of 1 h each demonstrate that photic input directly modulates activity levels in larvae. Larvae were monitored over a 24 h period (consisting of 12 cycles), with a series of twenty 400 ms video recordings taken every 10 min (offset from the beginning of each transition by 5 min). During light cycles, larvae were exposed to constant 60 μW cm^{-2}, while during dark cycles (shaded brown) larvae were maintained in darkness. (Di) The initiation frequency of both scoots and turns closely follows the light:dark cycle periodicity. Orange broken curves show functions estimated by performing non-linear regression according to the model: activity=b1+b2*sin(2π*time/b3+b4), such that b3 is the periodicity of the function (see text). (Dii) Mean initiation frequency for scoots (open circles) and turns (closed circles) for each time point during a 2 h period averaged over all 12 cycles. (E) Turn initiations show a transient increase for 5 s following the switch to sustained darkness (Ei, open circles, N=30 groups) compared to larvae maintained in constant illumination (200 μW cm^{-2}, closed circles, N=30 groups). No change in turn initiations occurs over the next 7 min. Immediately after light extinction, scoot initiations (Eii) are slightly reduced; however, after 60 s, scoots show a transient but highly significant increase above baseline levels. For each group of 400 ms recordings were collected at the indicated time points ($^{*}P$<0.05, t-test *versus* constant light). (F) Behavioral light adaptation begins 60 s after dark-adapted embryos are exposed to bright light (140 μW cm^{-2}, open circles, N=20 groups). After an initial spike in turns (Fi) elicited by the abrupt change in illumination, there is a lag of approximately 1 min in which turn initiations remain at similar levels to larvae maintained in constant darkness (closed circles, N=20 groups). Thereafter turn initiations rapidly climb to light-adapted levels. Scoot initiations (Fii) show a similar pattern, with an acute spike following light onset, a lag phase of 60 s, then a rapid increase to normal light-adapted levels ($^{*}P$<0.05, t-test *versus* constant dark).

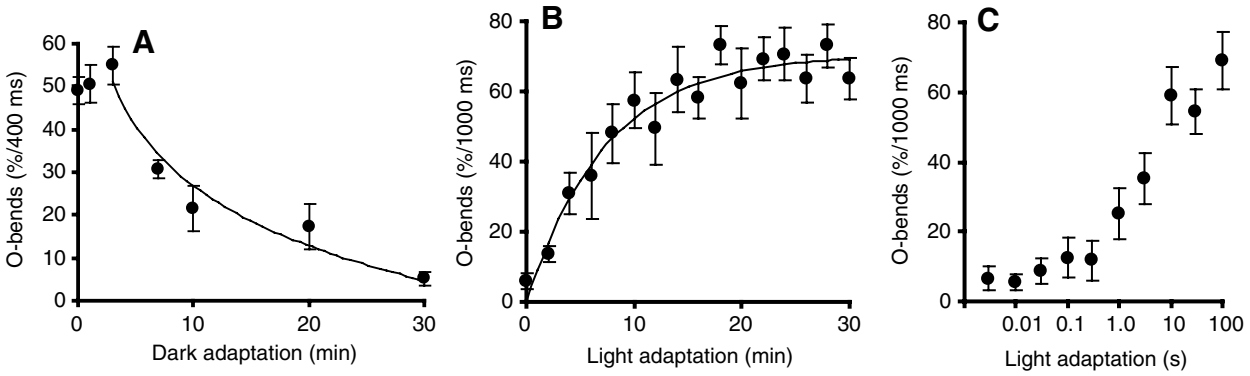

Fig. 7. Effect of light and dark adaptation on dark-flash responses. (A) Kinetics of behavioral dark adaptation assessed by responsiveness to dark flashes. Light-adapted larvae were placed in darkness, then tested at a single time point after the onset of dark adaptation (N=5 groups each time point). A test consisted of restoring the original level of illumination (200 μW cm^{-2}) and assessing responsiveness to a series of 5 dark flash stimuli of 500 ms duration, with 30 s intervals between stimuli. No change in dark-flash responsiveness is seen after 3 min of dark adaptation; however, exposure to longer periods of constant darkness rapidly reduces dark-flash responsiveness so that by 30 min, responsiveness to dark flashes is almost completely lost. (B) Kinetics of behavioral light adaptation assessed by responsiveness to dark flashes. Responsiveness to dark flashes develops slowly after dark-adapted larvae are exposed to constant bright light, reaching a maximum 20 min after the beginning of light adaptation. After the onset of illumination (400 μW cm^{-2}), groups (N=9) were tested with a 1000 ms long dark flash every 2 min. Video recordings were taken during the dark flash to measure O-bend responses. (C) Light-adapted larvae adjust quickly to increases in illumination. Larvae were pre-adapted at 10 μW cm^{-2} for at least 3 h, then shifted to 100 μW cm^{-2} for the indicated intervals before being tested with a 1000 ms dim flash back to 10 μW cm^{-2} (N=11 groups for each time point). After just 1 s of increased illumination, 25% of larvae respond to dim flashes with O-bend responses. Larvae reach maximal levels of responsiveness (70% of larvae, see Fig. 3D) to dim flashes after 100 s of sustained illumination.

responses differ from acoustic startle responses in lacking Mauthner cell dependence, and show distinct kinematic properties from routine turns, they constitute a novel motor pattern. We refer to these maneuvers as O-bends, reflecting the near circular shape achieved by the larvae, and their appearance during light-off stimuli (Fig. 4I).

Responses of larvae to dark/light adaptation

In mammals, diurnal control of locomotor activity is accomplished by two systems: an intrinsic circadian oscillator and 'masking responses' to absolute irradiance levels. We therefore sought to determine whether light intensity modulates locomotor activity in zebrafish larvae. Initiations of both scoots and turns significantly increased across 5 log units of light intensity (Fig. 6A; for turns, $F_{(5,54)}$=15.3, $P<10^{-10}$, for scoots $F_{(5,54)}$=15.6, $P<10^{-10}$). We next studied the behavior of larvae during adaptation to darkness. Larvae were pre-adapted to 200 μW cm^{-2} white light for at least 3 h before the onset of darkness. Initiations of scoots and turns did not decline after 5 min of dark adaptation, but dropped steadily over the next 30 min (Fig. 6B). After 30 min of dark adaptation initiations of both scoots and turns were significantly less than larvae maintained in constant illumination (scoots: 8.8% initiations per 400 ms window for control larvae *versus* 3.8% for dark adapted larvae; two-tailed t-test, P=0.011; turns: 10.3% for controls *versus* 4.1% in dark-adapted larvae; two-tailed t-test, P=0.014), reaching levels similar to those found in larvae maintained in constant darkness for several hours (compare time point –0.5 min in Fig. 6C). Decay time constants for turns and scoots were similar, 9.6 min and 11.9 min, respectively. In contrast, locomotor activity in larvae dark-adapted overnight increased very quickly after the onset of illumination (Fig. 6C), with scoot initiations reaching maximal levels 5 min after illumination and turn initiations reaching maximal levels after 15 min with a rise time constant of 4.1 min. After 30 min, initiations of scoots and turns in larvae exposed to illumination were very significantly greater than control larvae maintained in constant darkness (scoots: 3.0% initiations per 400 ms window for control larvae *versus* 9.5% for light-adapted larvae; two-tailed t-test, P<0.001. Turns: 2.4% for controls *versus* 13.8% in light-adapted larvae, two-tailed t-test P<0.001). These results show that locomotor activity in zebrafish larvae is modulated by the intensity of illumination.

Zebrafish larvae express rhythmic locomotor activity controlled by a circadian clock (Cahill et al., 1998; Prober et al., 2006). It is possible that the changes we observed in locomotor activity following light and dark shifts were secondary to phase shifting of the intrinsic oscillator. To address this possibility, we measured locomotor activity over 24 h using ultraradian cycles consisting of 1 h light and 1 h dark. Such short light:dark cycles preclude circadian entrainment in diverse species (Aschoff, 1999) including fish (Sanchez-Vazquez et al., 1996; Sanchez-Vazquez and Tabata, 1998). Consistent with activity levels being directly modulated by light, spectral analysis of the time series obtained revealed a harmonic peak for both scoots and turns at 121 min. Non-linear regression using a sinusoidal model confirmed that a significant component of variance in activity levels was accounted for by a periodic factor of close to 120 min (scoots: 119.9±0.91 min, r^2=0.510; turns: 120.6±1.08 min, r^2=0.427; estimate ±95% confidence interval). Thus, under such conditions, larvae exhibited cyclic motor activity, with initiations of both scoots and turns being maximal during light periods (Fig. 6Di). The mean frequency of turn initiations during light periods was 14.0±0.58% (per 400 ms window), significantly higher than the initiation frequency of 7.7±0.8% during dark periods (two-tailed t-test, $P<10^{-10}$). Scoot

initiations were 17.3±0.5% in light *versus* 9.4±0.5% during dark episodes (two-tailed *t*-test, $P<10^{-10}$). Combining data from all cycles confirmed that behavioral adaptation to onset of illumination is rapid, occurring within 5 min, whereas motor activity gradually declines starting 5–10 min after the onset of darkness (Fig. 6Dii). These results argue that the effect of light on activity levels in zebrafish larvae is direct, similar to masking stimuli in mammals.

We next sought to measure the kinetics of dark and light adaptation. Measurement of locomotor activity during the first 7 min of dark adaptation (Fig. 6E) showed that the initiation frequency of scoots was transiently elevated, peaking 1 min after dark adaptation (12.6% initiations per 400 ms window for controls in constant illumination *versus* 26.7% for larvae exposed to dark, two-tailed *t*-test, $P<10^{-4}$). Apart from the spike in turns in response to the change in illumination, turns remained constant over the first 7 min of dark adaptation. In contrast, measurement of locomotor activity in the first 7 min of light adaptation (Fig. 6F) demonstrated that after an acute spike in both scoots and turns provoked by the change in lighting, there was a lag phase of just 1 min before locomotor initiations rapidly increased to levels characteristic of light adapted larvae. After 2 min of light adaptation, initiations of both scoots and turns were significantly elevated above controls (scoots: 1.6% initiations per 400 ms window for controls in constant darkness *versus* 14.3% for larvae exposed to light; two-tailed *t*-test, $P=0.012$; turns: 1.1% for controls *versus* 11.9% for larvae exposed to light; two-tailed *t*-test, $P=0.0018$). Changes in locomotor activity during light and dark adaptation therefore have distinct time courses. Locomotor activity rapidly increases during light adaptation after a short lag phase. In contrast, dark adaptation triggers a biphasic behavioral program. For the first few minutes, net locomotor activity increases. After 5–10 min of constant darkness, locomotor activity begins to decline, reaching baseline levels within 30 min of the onset of darkness.

In the course of experiments, we noticed that dark-adapted larvae showed little responsiveness to dark flashes. This enabled us to measure the time course of acquisition or loss of responsiveness to dark flashes as an alternate measure of the kinetics of light and dark adaptation. Light-adapted larvae shifted to darkness did not lose responsiveness to dark flashes for the first 3 min, but thereafter rapidly lost responsiveness with a time constant of ~10 min (Fig. 7A). Thus, the temporal course of dark adaptation as assessed by locomotor activity and dark flash responsiveness is broadly similar.

During light adaptation from darkness, maximal dark-flash responsiveness was achieved after 20 min of light adaptation, with a time constant of ~7 min (Fig. 7B). In contrast, larvae already adapted to light quickly adjusted to brighter illumination. After a shift to more intense illumination, light adapted larvae responded to 'dim flashes' (down to the original level of illumination) after just 1 s of adaptation and reached maximal adaptation after 60 s (Fig. 7C). Thus the slow kinetics for recovery of O-bend responsiveness during adaptation from darkness cannot be accounted for by postulating that dark flash responsiveness is generally slow to adapt to changes in light levels. The differential time course of changes in locomotor activity and O-bend responsiveness during light adaptation from darkness argues that behavioral light adaptation is not a unitary process, but rather involves changes in several regulatory circuits.

Discussion

In the natural environment, fluctuations in lighting contain salient cues of both immediate and long-term significance. Here we show that zebrafish larvae respond to abrupt changes in illumination with acute motor responses and also integrate irradiance over longer time periods to regulate baseline levels of activity.

Analyzing larvae recorded in groups makes it possible to examine large numbers of motor events and facilitates quantitative analysis of behavior. A limitation of this technique is that the resolution of individual larvae is reduced and finer aspects of motor control cannot be examined. For example, we are not able to measure the contribution of pectoral fins to forward propulsion and braking (Budick and O'Malley, 2000; Thorsen et al., 2004), nor of fine tail movements for reorientation during predatory strikes (McElligott and O'Malley, 2005). A further limitation is that a single camera mounted from above can only record movements in the horizontal plane. On the other hand, automated measurement of behavior allows motor patterns to be classified on the basis of kinematic features. An observer-independent approach can reveal unanticipated motor patterns. The large turns recorded during dark flashes are kinematically distinct from other types of motor patterns involving turn movements, being large angle, but slow performance, suggesting that they form a distinct maneuver within the larval motor repertoire.

We found that zebrafish larvae show elevated locomotor activity during periods of bright illumination. This is likely to reflect a trade-off between requiring light to feed (Clark, 1981; Gahtan et al., 2005; McElligott and O'Malley, 2005) and the risk of predation. Thus, elevated locomotor activity in the light enlarges the area searched for food, while during darkness, when larvae do not efficiently feed, reduced locomotor activity minimizes the chances of encountering and attracting the attention of predators (Munk and Kiorboe, 1985). It is therefore advantageous for zebrafish larvae to synchronize activity levels to the diurnal cycle. The daily rhythm of activity in mammals is controlled by both the endogenous circadian system and external light cues (Aschoff, 1960). While circadian control of activity has been well documented in fish, fewer studies have explicitly addressed whether light stimuli can directly modulate fish behavior. Acute effects of light on adult fish behavior have been described for fry retrieval and fanning behavior (Reebs, 1994), feeding and locomotor activity (Sanchez-Vazquez et al., 1996; Sanchez-Vazquez and Tabata, 1998). Moreover, we interpret data in a recent study on hypocretin/orexin control of sleep/wake behavior in larval zebrafish as showing that light exposure during circadian night induces elevated locomotor activity [fig. 5D in Prober et al. (Prober et al., 2006)]. Our demonstration that light exposure directly modulates locomotor activity in larval zebrafish throughout the circadian cycle will facilitate molecular genetic analyses of masking responses.

Direct photic control of activity may serve to fine-tune the inaccurate free-running circadian periods measured in a variety of fish species including larval zebrafish (Cahill et al., 1998;

Hurd and Cahill, 2002). In larval zebrafish, locomotor activity is subject to circadian control from the onset of spontaneous movement at day 4, with maximal activity during early subjective day (Hurd and Cahill, 2002). Our results demonstrate that, as in mammals, light/dark cues can override activity levels set by the endogenous clock. In mammals such masking stimuli are most effective when they coincide with the activity period set by the circadian clock (Aschoff, 1999; Redlin and Mrosovsky, 1999). Further experiments will be required to determine whether masking stimuli and circadian rhythms interact in a similar way in larval zebrafish.

Following the onset of darkness, larvae showed a transient elevation in scoots prior to a gradual drop-off in motor activity. As many diurnal fish species engage in cover-seeking activity at dusk (Helfman, 1986), it is possible that the hyperactivity we observed is aimed at finding shelter prior to night. However, the onset of night is not the only condition in which a larva may find itself in darkness. Accidental navigation under debris may also occlude light. Dark induced hyperactivity may therefore serve to facilitate navigation back to areas of illumination if the darkness is not due to nightfall.

We propose that the O-bend responses to dark flashes may also serve to maintain larvae in well-lit environments. An alternative hypothesis is that abrupt reductions in illumination represent the shadow of a potential predator, and that the large angle turns elicited are a precursor to the adult zebrafish visual startle response (Easter and Nicola, 1997). Two lines of evidence argue that O-bend responses are navigational rather than defensive. First, we found that responses to light occlusion are made towards the direction of the occluded light. This would displace the larva towards a potential predator. In contrast, escape trajectories in adult fish displace fish away from predators (Dill, 1974; Domenici, 2002). The visual startle response in adult fish is generally elicited using a looming stimulus in which rapid expansion of an object in the visual field simulates predator approach. Zebrafish larvae also respond to looming stimuli by turning away from the potential threat (H.A.B. and M.G., unpublished). It therefore seems unlikely that larvae interpret sudden light occlusion as a potential threat. Instead, a rapid drop in light intensity may constitute a distinct cue occurring when a larva strays into a shaded environment. A 180° turn would reorient the larva towards the well-lit region from which it came.

Second, stimulation of the optic nerve in adult fish can bring the Mauthner cell to threshold (Zottoli et al., 1987) and visual stimuli can elicit C-starts with similar kinematics to acoustic/vibrational startle responses (Dill, 1974; Eaton et al., 1977). Our data show that larval responses to abrupt light decrements are not mediated by the Mauthner cell and show distinct kinematics from acoustic startle responses. Dark-flash responses have a broad latency distribution, with responses often being initiated several hundred ms after the stimulus. By comparison, acoustic startle latencies in larvae range from 4–12 ms. The long latency and slow performance of responses to sudden light occlusion are inconsistent with a primarily defensive role. Escape responses to head-touch stimuli in larval zebrafish are mediated by the Mauthner cell together with its segmental homologs (Liu and Fetcho, 1999). Although we cannot exclude the possibility that the Mauthner homologs mediate dark-flash responses, escape responses initiated by these neurons have much greater angular velocity than dark-flash responses. It is likely that O-bend responses are triggered by a distinct cohort of reticulospinal neurons. Thus, in contrast to previous proposals that the larval ‘visual startle’ response is the precursor to the adult zebrafish escape response (Easter and Nicola, 1997), we suggest that O-bend responses are not mediated by the Mauthner circuit, are primarily navigational, and constitute one of several mechanisms by which zebrafish larvae maintain themselves in an illuminated region conducive to successful feeding.

Prolonged dark adaptation had two behavioral effects, reducing locomotor activity and eliminating dark-flash responsiveness. The kinetics of dark adaptation were similar for these two processes. Both behaviors were maintained for the first 3 min of darkness then declined over the course of 30 min. In contrast the time course for recovery of responsiveness to dark flashes during light adaptation (time constant=7 min) is slower than the recovery of locomotor activity (turns; time constant=4 min) or recovery of the optokinetic response (time constant=3 min) (Page-McCaw et al., 2004). A variety of mechanisms operating on different timescales are known to participate in light adaptation (Dunn and Rieke, 2006; Pugh et al., 1999). Thus, the rapid normalization of sensitivity to dark flashes after a shift to higher light levels may involve biochemical processes in photoreceptors such as phosphorylation of cone opsins (Kennedy et al., 2004), whereas retinal network and possibly central adaptations are likely involved in the slower adjustments to and from darkness.

Work on behavioral choice in invertebrates is beginning to shed light on how the nervous system produces behavior. One reason for the productivity of these studies has been the focus on describing circuits that activate intrinsic and stereotyped motor patterns (Briggman et al., 2005; Gray et al., 2005). Goal-directed behaviors are then understood as the outcome of sequential activation of elements of the motor repertoire. Here we take a similar approach in a vertebrate model, the larval zebrafish, showing that motor patterns can be reliably measured and distinguished. Visual stimuli differentially activate and modulate elements of the motor repertoire. Following light extinction, larvae execute large angle turn responses toward the vanished light source, then show transient locomotor activation before slowly settling into a hypoactive state. After the onset of illumination, larvae rapidly increase baseline activity levels. We propose that these patterns of motor activation all serve to maximize time spent in well-lit environments suitable for feeding. These results provide a foundation for future studies examining neural mechanisms controlling the expression of motor patterns in larval zebrafish.

We thank Dr M. Halpern and members of the Granato laboratory for helpful discussions and advice on the manuscript. This work was supported by an NRSA postdoctoral fellowship to H.A.B. and grants from the National Institute of Health (MH075691 and HD 37975) to M.G.

References

Aschoff, J. (1960). Exogenous and endogenous components in circadian rhythms. *Cold Spring Harb. Symp. Quant. Biol.* **25**, 11-28.

Aschoff, J. (1999). Masking and parametric effects of high-frequency light-dark cycles. *Jpn. J. Physiol.* **49**, 11-18.

Borla, M. A., Palecek, B., Budick, S. and O'Malley, D. M. (2002). Prey capture by larval zebrafish: evidence for fine axial motor control. *Brain Behav. Evol.* **60**, 207-229.

Briggman, K., Abarbanel, H. and Kristan, W., Jr (2005). Optical imaging of neuronal populations during decision-making. *Science* **307**, 896-901.

Brockerhoff, S., Hurley, J., Janssen-Bienhold, U., Neuhauss, S., Driever, W. and Dowling, J. (1995). A behavioral screen for isolating zebrafish mutants with visual system defects. *Proc. Natl. Acad. Sci. USA* **92**, 10545-10549.

Brockerhoff, S., Hurley, J., Niemi, G. and Dowling, J. (1997). A new form of inherited red-blindness identified in zebrafish. *J. Neurosci.* **17**, 4236-4242.

Budick, S. and O'Malley, D. (2000). The behavioral repertoire of larval zebrafish: swimming, escaping and prey capture. *J. Exp. Biol.* **203**, 2565-2579.

Cahill, G., Hurd, M. and Batchelor, M. (1998). Circadian rhythmicity in the locomotor activity of larval zebrafish. *NeuroReport* **9**, 3445-3449.

Clark, D. T. (1981). Visual responses in developing zebrafish (*Brachydanio rerio*). PhD dissertation, University of Oregon, USA.

Crocker, J. and Grier, D. (1996). Methods of digital video microscopy for colloidal studies. *J. Colloid Interface Sci.* **179**, 298-310.

Dill, L. (1974). The escape response of the zebra danio (*Brachydanio rerio*). I. The stimulus for escape. *Anim. Behav.* **22**, 710-721.

Domenici, P. (2002). The visually mediated escape response in fish: predicting prey responsiveness and the locomotor behaviour of predators and prey. *Mar. Freshw. Behav. Physiol.* **35**, 87-110.

Dunn, F. A. and Rieke, F. (2006). The impact of photoreceptor noice on retinal gain controls. *Curr. Opin. Neurobiol.* **16**, 363-370.

Easter, S. and Nicola, G. (1997). The development of vision in the zebrafish (*Danio rerio*). *Dev. Biol.* **180**, 646-663.

Eaton, R. C., Bombardieri, R. A. and Meyer, G. (1977). The mauthner-initiated startle response in teleost fish. *J. Exp. Biol.* **66**, 65-81.

Gahtan, E., Tanger, P. and Baier, H. (2005). Visual prey capture in larval zebrafish is controlled by identified reticulospinal neurons downstream of the tectum. *J. Neurosci.* **25**, 9294-9303.

Gray, J. M., Hill, J. J. and Bargmann, C. I. (2005). A circuit for navigation in *Caenorhabditis elegans*. *Proc. Natl. Acad. Sci. USA* **102**, 3184-3191.

Hatta, K. (1992). Role of the floor plate in axonal patterning in the zebrafish CNS. *Neuron* **9**, 629-642.

Hattar, S., Lucas, R., Mrosovsky, N., Thompson, S., Douglas, R., Hankins, M., Lem, J., Biel, M., Hofmann, F. and Foster, R. (2003). Melanopsin and rod–cone photoreceptive systems account for all major accessory visual functions in mice. *Nature* **424**, 75-81.

Helfman, G. S. (1986). Fish behaviour by day, night and twilight. In *The Behavior of Teleost Fishes* (ed. T. J. Pitcher), pp. 366-387. Baltimore: The Johns Hopkins University Press.

Hopf, H. D., Bier, J., Breurer, B. and Scheerer, W. (1973). The blink reflex induced by photic stimuli: parameters, thresholds and reflex times. In *New Developments in Electromyography and Clinical Neurophysiology*. Vol. 3 (ed. J. E. Desmedt), pp. 666-672. Basel: Karger.

Hurd, M. and Cahill, G. (2002). Entraining signals initiate behavioral circadian rhythmicity in larval zebrafish. *J. Biol. Rhythms* **17**, 307-314.

Keeler, C. (1927). Iris movements in blind mice. *Am. J. Physiol.* **81**, 107-112.

Kennedy, M., Dunn, F. and Hurley, J. (2004). Visual pigment phosphorylation but not transducin translocation can contribute to light adaptation in zebrafish cones. *Neuron* **41**, 915-928.

Kimmel, C. B., Patterson, J. and Kimmel, R. O. (1974). The development and behavioral characteristics of the startle response in the zebra fish. *Dev. Psychobiol.* **7**, 47-60.

Klein, D. and Weller, J. (1972). Rapid light-induced decrease in pineal serotonin N-acetyltransferase activity. *Science* **177**, 532.

Kristan, W., Jr and Shaw, B. (1997). Population coding and behavioral choice. *Curr. Opin. Neurobiol.* **7**, 826-831.

Lewy, A., Wehr, T., Goodwin, F., Newsome, D. and Markey, S. (1980). Light suppresses melatonin secretion in humans. *Science* **210**, 1267.

Liu, K. S. and Fetcho, J. R. (1999). Laser ablations reveal functional relationships of segmental hindbrain neurons in zebrafish. *Neuron* **23**, 325-335.

McElligott, M. and O'Malley, D. (2005). Prey tracking by larval zebrafish: axial kinematics and visual control. *Brain Behav. Evol.* **66**, 177-196.

Muller, U. and van Leeuwen, J. (2004). Swimming of larval zebrafish: ontogeny of body waves and implications for locomotory development. *J. Exp. Biol.* **207**, 853-868.

Munk, P. and Kiorboe, T. (1985). Feeding behaviour and swimming activity of larval herring (*Clupea harengus*) in relation to density of copepod nauplii. *Mar. Ecol. Prog. Ser.* **24**, 15-21.

Neuhauss, S. (2003). Behavioral genetic approaches to visual system development and function in zebrafish. *J. Neurobiol.* **54**, 148-160.

Orger, M. and Baier, H. (2005). Channeling of red and green cone inputs to the zebrafish optomotor response. *Vis. Neurosci.* **22**, 275-281.

Ouagazzal, A., Jenck, F. and Moreau, J. (2001). Drug-induced potentiation of prepulse inhibition of acoustic startle reflex in mice: a model for detecting antipsychotic activity? *Psychopharmacology* **156**, 273-283.

Page-McCaw, P., Chung, S., Muto, A., Roeser, T., Staub, W., Finger-Baier, K., Korenbrot, J. and Baier, H. (2004). Retinal network adaptation to bright light requires tyrosinase. *Nat. Neurosci.* **7**, 1329-1336.

Panda, S., Provencio, I., Tu, D., Pires, S., Rollag, M., Castrucci, A., Pletcher, M., Sato, T., Wiltshire, T. and Andahazy, M. (2003). Melanopsin is required for non-image-forming photic responses in blind mice. *Sci. STKE* **301**, 525-527.

Prober, D. A., Rihel, J., Onah, A. A., Sung, R.-J. and Schier, A. F. (2006). Hypocretin/orexin overexpression induces an insomnia-like phenotype in zebrafish. *J. Neurosci.* **26**, 13400-13410.

Pugh, E., Jr, Nikonov, S. and Lamb, T. (1999). Molecular mechanisms of vertebrate photoreceptor light adaptation. *Curr. Opin. Neurobiol.* **9**, 410-418.

Redlin, U. (2001). Neural basis and biological function of masking by light in mammals: suppression of melatonin and locomotor activity. *Chronobiol. Int.* **18**, 737-758.

Redlin, U. and Mrosovsky, N. (1999). Masking of locomotor activity in hamsters. *J. Comp. Physiol. A* **184**, 429-437.

Reebs, S. G. (1994). The anticipation of night by fry-retrieving convict cichlids. *Anim. Behav.* **48**, 89-95.

Samuel, A. and Sengupta, P. (2005). Sensorimotor integration: locating locomotion in neural circuits. *Curr. Biol.* **15**, 341-343.

Sanchez-Vazquez, F. and Tabata, M. (1998). Circadian rhythms of demand-feeding and locomotor activity in rainbow trout. *J. Fish Biol.* **52**, 255-267.

Sanchez-Vazquez, F., Madrid, J., Zamora, S., Iigo, M. and Tabata, M. (1996). Demand feeding and locomotor circadian rhythms in the goldfish, *Carassius auratus*: dual and independent phasing. *Physiol. Behav.* **60**, 665-674.

Stahl, B. (1977). Early and recent primitive brain forms. *Ann. N. Y. Acad. Sci.* **299**, 87-96.

Thorsen, D., Cassidy, J. and Hale, M. (2004). Swimming of larval zebrafish: fin-axis coordination and implications for function and neural control. *J. Exp. Biol.* **207**, 4175-4183.

Yates, S. (1981). Light-stimulus-evoked blink reflex: methods, normal values, relation to other blink reflexes, and observations in multiple sclerosis. *Neurology* **31**, 272-281.

Zottoli, S., Hordes, A. and Faber, D. (1987). Localization of optic tectal input to the ventral dendrite of the goldfish Mauthner cell. *Brain Res.* **401**, 113-121.